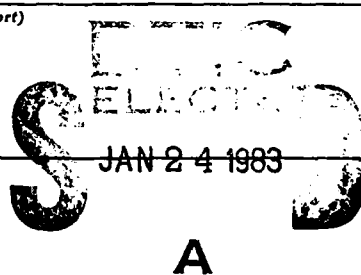


MICROCOPY RESOLUTION TEST CHART  
NATIONAL BUREAU OF STANDARDS-1963-A

5

REPORT DOCUMENTATION PAGE		READ INSTRUCTIONS BEFORE COMPLETING FORM	
1. REPORT NUMBER	2. GOVT ACCESSION NO.	3. RECIPIENT'S CATALOG NUMBER	
	ADA 123693		
TITLE (and Subtitle)		5. TYPE OF REPORT & PERIOD COVERED	
The role of hydrogen in the stress corrosion failure of high strength Al-Zn-Mg alloys		Annual Technical Report September 1980-October 1982	
AUTHOR(s)		6. PERFORMING ORG. REPORT NUMBER	
M. L. Yuen and H.M. Flower			
PERFORMING ORGANIZATION NAME AND ADDRESS		8. CONTRACT OR GRANT NUMBER(s)	
Imperial College of Science and Technology South Kensington London SW7 2AZ		DAJA 37-80-C-0372	
CONTROLLING OFFICE NAME AND ADDRESS		10. PROGRAM ELEMENT, PROJECT, TASK AREA & WORK UNIT NUMBERS	
USARDSG-UK Box 65 FPO New York 09510		61102A IT161102BH57-04	
MONITORING AGENCY NAME & ADDRESS (if different from Controlling Office)		12. REPORT DATE	
		October 1982	
		13. NUMBER OF PAGES	
		22	
		15. SECURITY CLASS. (of this report)	
		Unclassified	
		15a. DECLASSIFICATION/DOWNGRADING SCHEDULE	
16. DISTRIBUTION STATEMENT (of this Report)			
Approved for public release; Distribution unlimited.			
17. DISTRIBUTION STATEMENT (of the abstract entered in Block 20, if different from Report)			
			
18. SUPPLEMENTARY NOTES			
19. KEY WORDS (Continue on reverse side if necessary and identify by block number)			
Aluminium. Brittle fracture. Electron microscopy. Fractography Hydrogen embrittlement. Hydrogen trapping. Pre-exposure. Slow strain rate testing. Stress corrosion.			
20. ABSTRACT (Continue on reverse side if necessary and identify by block number)			
Three alloys, Al 6% Zn 3% Mg. Al 6% Zn 3% Mg 1.7% Cu and Al 6% Zn 3% Mg 0.14% Cr. were pre-exposed in the solution treated condition to water vapour at 115°C. Dry control tests were also performed. Both sets of samples were tested in tension using a slow strain rate of $10^{-6} \text{ s}^{-1}$ and the results were compared with previously obtained data using a strain rate of $10^{-3} \text{ s}^{-1}$ . All the samples exposed to steam showed evidence of hydrogen embrittlement, the effects being more severe at the slow strain rate. Evidence was also obtained for hydrogen embrittlement via reaction of the			

UNCLASSIFIED

SECURITY CLASSIFICATION OF THIS PAGE(When Data Entered)

metal with the laboratory air during slow strain rate testing in all cases except for the copper containing alloy. Both intergranular and transgranular brittle fracture can be produced as a result of hydrogen absorption into the metal: tolerance to hydrogen is related to the ability of the microstructure to trap hydrogen in the form of gas bubbles.

UNCLASSIFIED

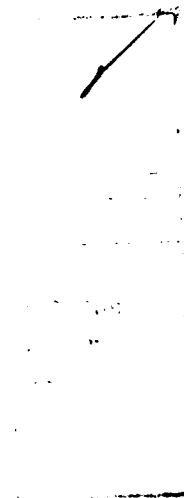
SECURITY CLASSIFICATION OF THIS PAGE(When Date Entered)

C O N T E N T S

	Page
1. Introduction	1
2. Experimental procedure	1
3. Results	4
4. Discussion	10
5. Conclusions and proposals	13
References	
Figures	
Photographs	



A



## 1. INTRODUCTION

The role of hydrogen in the environmental failure of Al-Zn-Mg alloys was investigated under a previous U.S. Army contract no. DA-ERO-77-G-11, (1). The changes in mechanical properties and microstructures observed during elevated-temperature exposure to water vapour can be explained in terms of hydrogen embrittlement. On grain boundaries and in the grain matrix, hydrogen is capable of causing grain boundary decohesion or transgranular cleavage respectively. On suitable sites, e.g. precipitates or grain boundaries, hydrogen recombines to form bubbles, depleting the surrounding matrix of dissolved hydrogen; this raises the total intake of hydrogen before failure takes place. The addition of copper or chromium improves hydrogen embrittlement resistance, either by activating hydrogen recombination or by inhibiting hydrogen entry and by refining the grain size.

Atomic hydrogen, as a by-product of hydration, diffuses along grain boundaries and through the matrix by normal diffusion mechanisms or by transport by dislocations during plastic deformation (2-5). Lowering the strain rate in a tensile test allows more time for injecting fresh hydrogen and redistributing that which already exists (4). If testing is carried out on samples previously exposed to water vapour, hydrogen can be redistributed to local stress concentrations which causes local enhancement of embrittlement and results in a lower overall tensile elongation. To study the environmental effects on these alloys time must be allowed for the embrittlement process to take place. This is achieved either by exposing the sample in an aggressive environment prior to testing (pre-exposure) or by testing the sample in the aggressive environment over a long period of time. (The latter refers to stress corrosion tests, i.e. testing under the combined effect of stress and corrosion.)

The conventional methods are to test specimens under constant stress (or load) or under constant strain in an aggressive environment. They are usually very time-consuming (up to months), and are very difficult to monitor with regard to deformation rate. In practice, to minimise the test time, the environmental

become unrealistic and the information obtained may be inadequate.

Most slow strain rate tests are held in an environmental cell using a conventional testing machine with modified speed reducer to provide a slow constant overall strain rate. If the strain rate is too high, the specimen will fail mechanically without any environmental influence. If the strain rate is too low, corrosion may produce a protective passive film and embrittlement is ineffective. There is a critical strain rate range within which the specimen is embrittled by the test environment (6-8). Such slow strain rate techniques can easily achieve natural crack growth rates of the range of  $10^{-6} - 10^{-9} \text{ ms}^{-1}$ . These techniques reduce test time to days or hours. They provide more quantitative information and they can also show up the ranking of environmental susceptibility of certain alloys, e.g. Cr-steels which otherwise do not respond to conventional tests (8). However, slow strain rate techniques still cannot control rapid increases of local plastic deformation which has started or been initiated by a crack. The resulting local strain rate may rise above the critical strain rate range and embrittlement will not be observed.

Despite the problem of uncontrollable local strain rate, slow strain rate techniques provide more reliable information in a shorter period of time than conventional stress corrosion test methods. For these reasons, the Al-Zn-Mg-based alloys examined under the previous contract have been studied using the slow strain rate technique.

## 2. EXPERIMENTAL PROCEDURE

The composition of the 3 alloys investigated are given below (1):

Alloy	Cr	Cu	Fe	Mg	Mn	Si	Ti	Zn	
High Purity base (6/3)	0.01	0.002	0.01	2.9	0.002	0.01	0.01	6.1	Balance Al
Cu containing experimental alloy (6/3 Cu)	0.001	1.7	0.02	3.0	0.001	0.01	0.01	6.3	
Cu containing experimental	0.14	0.002	0.01	2.99	-	0.01	-	6.11	

## 2.1. Preparation

25mm slabs were cut from the ingots. They were rolled down to a thickness of 0.5mm. Frequent anneals at 450°C were required to prevent bending or cracking of the sheets because of the fast work-hardening rates experienced.

Flat tensile specimens of thickness approximately 0.5mm, with a gauge length of 22mm and gauge width of 6mm were stamped parallel to the rolling direction. They were cleaned in 20% NaOH at 70°C. The black oxide so produced was removed in dilute HNO<sub>3</sub> and the samples were rinsed in successive baths of distilled water. They were finally degreased in inhibisol in an ultrasonic cleaner.

All samples were solution-treated at 450°C  $\pm$  3°C for an hour in a dry argon atmosphere in a horizontal furnace. After cold water quenching, they were kept dry except during experimental exposure.

To test whether mechanical properties were affected by surface finish, some specimens were polished before cleaning in NaOH. It was found that the samples which had been polished produced no significant improvement in tensile strength and ductility and therefore no further polishing was carried out.

## 2.2 Heat treatment

Samples were pre-exposed at 115°C in an autoclave at a steam pressure of 1.75 bar. Dry control samples, sealed in pyrex tubes, were heat-treated alongside the exposed samples for various periods up to 435 hours. Distilled water was used in the exposure to eliminate any effect of impurities present in tap water. After exposure, samples were tested immediately or stored in liquid nitrogen at -196°C to avoid outgassing. Control samples were kept in a dessicator if an immediate test was not possible. At least 2 samples were tested for each condition.

Ageing the samples at 115°C (as in this study) or at 120°C (as in the previous study (1)) should produce identical microstructures for the same ageing periods; thus slow strain rate results here are directly comparable with the fast strain



rate results from the previous investigation (1).

### 2.3 Mechanical tests.

Tensile tests were carried out using an Instron machine, mostly at a cross-head speed of 0.0005 cm per minute, equivalent to a strain rate of about  $4 \times 10^{-6}$  per second. A few samples were tested at a higher strain rate to ensure that embrittlement did not arise from undesirable exposure due to mishandling. In every test the entire sample was enclosed in a perspex cell containing fresh silica gel. This provided a standard dry environment. However, tensile tests of control dry samples showed evidence of embrittlement (see below) as a result of the reaction of the samples with the moisture retained in the cell. The dry environment provided by the fresh silica gel was inefficient and thus the tests were in effect held in laboratory air.

### 2.4 Fractography

Fracture surfaces were gold-coated and examined using a JEOL JSM T200 scanning electron microscope.

### 2.5 Transmission electron microscopy (TEM)

Discs were punched from the gauge (near fracture region) and grip. They were ground down so that some foils were in the sample surface vicinity and others in the centre of the section. Thin foils were prepared using a Struers electro-polishing machine in 20% nitric acid in methanol at  $-20^{\circ}\text{C}$ , at a voltage of 15V. They were examined using the Phillips F1 301; fresh samples and foils were needed to see  $\text{H}_2$  bubbles since hydrogen is not retained in thin foils for periods of more than a few hours.

## 3. RESULTS

The tensile test results - elongation (%), 0.2% proof stress and fracture stress, are plotted in Figs. 1, 2, 4, 5, 7, and 8, where high strain rate results (1)

are available. They are shown on the transparent overlay for comparison and the results are tabulated.

A considerable number of fracture samples examined showed evidence of non-uniform strain rate during failure. One end of the sample had intergranular or brittle fracture and the amount of ductile appearance increased across the width of the sample (photos 1a, b and c). Cracks nucleated and, initially, propagated at slow strain rates. Crack opening was assisted by the weakening of bonds due to the presence of hydrogen. The precise mechanism of such an embrittlement is uncertain; dissolved hydrogen is presumed to cause a reduction in grain boundary surface energy which leads to grain boundary decohesion (1). When the remaining area could not support the load it failed at higher strain rates and thus showed more ductile fractures. In order to show the relationship of slow strain rate with hydrogen embrittlement, only slow strain rate fracture regions are summarised in Figs. 3, 6 and 9a. The fast strain rate test fractography results (1) are also shown in Figs. 3, 6 and 9b for comparison.

Thin foils prepared from gauge, grip, surface or interior showed no microstructural difference. Since few fresh foils were available for observation, it is assumed that all H<sub>2</sub> bubble formation conditions are identical to those observed by Christodoulou unless otherwise stated.

### 3.1 Ternary alloy Al-Zn-Mg.

#### 3.1.1 Slow strain rate test. (see separate sheet overleaf)

#### 3.1.2 Fractography.

See Figs. 3a and b. A few fracture samples were kept in laboratory air for a month before examination. The grain boundaries on the exposed fracture surface became badly blistered by reaction with the air. Photo 2 shows the cracking of some blisters from hydrogen pressure build up. No such fracture was observed on the sides of the fracture samples. This indicates the moisture level of laboratory air and the highly active state of the grain boundary fracture

3.1.1. Slow strain rate test.

Parameter change with time	Slow strain rate $4 \times 10^{-6} \text{ s}^{-1}$		Fast strain rate $4 \times 10^{-3} \text{ s}^{-1}$	
	Wet	Dry	Wet	Dry
Elongation	Rapid decrease to 0-1% in 5 hours	Gradual decrease to 0-1% in 30 hrs.	Gradual decrease followed by abrupt recovery at 24-35 hrs. then zero ductility	Gradual decrease due to age hardening.
	Wet < dry by very little			
Large amount of H injected during slow strain rate test. Thus wet and dry samples had little difference while comparing slow and fast strain rate; slow samples showed more embrittlement.				
0.2% Proof stress	About $250-300 \text{ MNm}^{-2}$		-	
Fracture stress	Wet < dry by $50 \text{ MNm}^{-2}$ to $350 \text{ MN}^{-2}$		Maximum of $450 \text{ MN}^{-2}$	-
At slow strain rate, high concentration of H ahead of the crack tip lowered the strength dramatically				

See Figs. 1, 2 a, b.

3.2 Copper-bearing Al-Zn-Mg-Cu

3.2.1 Slow strain rate test

Parameters change with time	Slow strain rate $4 \times 10^{-6} \text{ s}^{-1}$		Fast strain rate $4 \times 10^{-3} \text{ s}^{-1}$	
	Wet	Dry	Wet	Dry
Elongation	Rapid decrease from age hardening and pre-exposure but the effect saturates after 80 hrs. to 3-4% of elongation	Rapid decrease from age hardening. Little change after 20 hrs with elongation $\sim$ 6-8%	No embrittlement from pre-exposure, elongation about 8%	
Lowering strain rate raises H level in the pre-exposure samples and reduces their elongation. However, it has only slight effect on dry samples.				
0.2% proof stress	About 380-420 $\text{MNm}^{-2}$		-	
Fracture stress	Pre-exposure lowers fracture stress by about 50 $\text{MNm}^{-2}$ to 550 $\text{MNm}^{-2}$		-	
It is believed that lowering the strain rate reduces fracture stress.				

See Figs. 4a, b, and 5.

3.2.2 Fractography.

See Fig. 6 a and b. Samples exposed for a short time had a confined peripheral region which was severely intergranularly embrittled. The centre was ductile with some cleavage detectable adjacent to the embrittled edge. Prolonged exposure spread the region of intergranular embrittlement throughout the sample thickness. The three regions of fracture, ie the intergranular periphery, the transgranular cleavage and the transgranular ductile centre; were also observed in higher strain-rate tests in the range of 20-90 hours of pre-exposure (1). The use of slow strain rates enhanced such failure with 3 regions of fracture in even shorter pre-exposure times as a result of embrittlement during testing.

In these slow strain rate tests, the higher strain rate regions which failed last also showed 3 regions of fracture (intergranular, cleavage and ductile) in both wet and dry samples. The appearance of each region and the fraction each mode

occupied over the fracture surface, were very dependent on the actual local strain rate which makes detailed interpretation of fractography difficult; however, there is a trend of reduction in ductile appearance with long exposure or ageing time.

### 3.2.3 TEM.

The precipitation and H<sub>2</sub> bubble formation are expected to be the same as was observed in the previous investigation (1), i.e.

- (1) addition of copper promotes precipitation along grain boundaries in the grain matrix;
- (2) H<sub>2</sub> bubble formation starts at 20 hours exposure or even earlier.

Present observations show the presence of H<sub>2</sub> bubbles along grain boundaries and also on dislocation bands inside the grain matrix, (see photo. 3). It is therefore clear that large concentrations of hydrogen can be injected not only into grain boundaries but also into grain interiors. The relatively high ductility associated with this condition indicates a high tolerance to hydrogen which is presumably associated with the relative ease with which hydrogen is trapped in the bubbles which readily nucleate in this alloy.

## 3.3 Chromium-bearing Al-Zn-Mg-Cr

### 3.3.1 Slow strain rate test (See separate sheet overleaf.)

### 3.3.2. Fractography.

See Figs. 9a and b. The fracture surface of the wet samples pre-exposed up to 40 hours was brittle intergranular, (photo 4a). As pre-exposure time increased, the fracture surfaces consisted of the 3 regions, i.e. brittle intergranular rim, cleavage and ductile central core. The fracture surfaces of the dry samples changed from the 3 regions of fracture (up to 6 hours of ageing) to ductile intergranular grain boundary decohesion (photo 4b). Beyond 120 hours ageing, the fracture surface was ductile transgranular again. This anomalous sequence can

3.3.1 Slow strain rate test.

Parameter change with time	Slow strain rate		Fast strain rate	
	Wet	Dry	Wet	Dry
Elongation	After initial decrease from age hardening and pre-exposure, effect saturates to give ~ 1%	After initial decrease to 2% age softening raised the elongation to ~ 4-6%	Slow embrittling effect ~ 6-8%	Slow age hardening followed by over ageing ~ 10%
	Slow strain rate induced HE but the effect saturated after certain pre-exposure or ageing period			
0.2% proof stress	About 420 MNm <sup>-2</sup>		-	
Fracture stress	Pre-exposure lowers fracture stress by 40 MNm <sup>-2</sup>		-	
	Slow strain rate is believed to lower stress by weakening bonding around cracking tip, i.e. HE.			

See Figs. 7 a, b, and 8.

be explained in terms of ageing, pre-exposure and hydrogen embrittlement during slow straining (see below). In spite of the more ductile appearance of the wet samples, they had more sub-microscopic intergranular cracks than the dry samples.

### 3.3.3 TEM

H<sub>2</sub> bubbles were observed on precipitates on grain boundaries in bulk samples exposed for 192 hours (photo 5).

## 4. DISCUSSION

The effects of pre-exposure on the alloys are shown by the fast strain rate results. Embrittlement during slow strain rate tests caused by the rapid hydrogen transport via mobile dislocations can be more detrimental. Estimates of the hydrogen penetration depth via dislocation sweeping is several orders of magnitude higher than via lattice diffusion paths (9). The amount of hydrogen injected into a sample depends on the time from yield to failure, ie. when dislocations are mobile. This duration is related to the following:

- (1) the intrinsic ductility of the sample itself - affected by ageing and pre-exposure;
- (2) the hydrogen embrittlement during straining - the more intrinsically ductile the sample, the longer the test time and the longer the time available for dynamic hydrogen embrittlement. On the other hand, a brittle sample is less affected by dynamic hydrogen embrittlement.

Thus lowering the strain rate has little effect on already-brittle materials but will reduce the ductility of intrinsically ductile conditions. However, in the absence of environmental effects e.g. if the test is held under vacuum or in an inert atmosphere, lowering the strain rate allows the sample to flow plastically under a lower stress. This results in a higher ductility (7,10).

Photos la, b and c are the fractographs along the width of a dry ternary sample aged for 4 hours. (a) is one end of the sample where a crack initiated at lower

strain rate. A large quantity of hydrogen was injected at the crack tip and therefore it failed by grain boundary decohesion. As the crack propagated, the strain was increased locally; it allowed less time for hydrogen injection and thus (b) shows more ductile appearance. Finally, the sample could not sustain the load and failed at much higher strain rates. (c) is the other end of the sample which had suffered little or no hydrogen embrittlement. Thus (a), (b) and (c) show the increasingly ductile appearance along the width of the tensile sample as local strain rate increased and hydrogen embrittlement diminished throughout the failure of the sample.

Slow straining had the worst effect in the ternary alloy. The large grain size and poor hydrogen trapping efficiency allowed rapid hydrogen transport by diffusion and dislocation sweeping. The injection and redistribution of hydrogen ahead of the crack tip enabled it to propagate at lower stresses, explaining why the ductility recovery observed in samples exposed for 24-36 hours and tested at high strain rates (1), was not experienced in the slow strain rate tests and why in general, specimens had a more brittle fracture appearance than the corresponding fast strain rate samples. However, beyond 36 hours of pre-exposure, the highly brittle state of the samples allowed little time for dynamic hydrogen embrittlement. Effectively, these tests were unaffected by the test environment and the samples therefore benefited by slow straining. Up to 40 hours of pre-exposure (longer exposure times have not been carried out) led to fractography showing multiple slip steps whereas the fast strain rate samples were fully brittle.

The elongation of the copper-bearing alloy was not diminished by pre-exposure or by slow straining (see Fig.4 a and b). However, fractographic observation revealed that the slow strain rate enhanced pre-exposure embrittlement due to hydrogen redistribution. On the other hand, fractography of dry samples showed ductile transgranular fracture while the fracture surfaces of fast-strain-rate samples were ductile intergranular. Again, the dry samples benefited from the 'creep' effect from slow straining which implies that hydrogen injection during slow straining was slow, or that the copper-bearing alloy provided good hydrogen traps and H<sub>2</sub> recom-



Elongation and fractography of both wet and dry chromium-bearing samples were affected by slow straining. The effect of pre-exposure was enhanced as elongation was reduced from 7% in the fast strain rate tests, to 1-2% in the slow strain rate tests. The amount of hydrogen diffused into the samples pre-exposed up to 40 hours was not very large. During the 6 hours of slow straining, the dissolved hydrogen and freshly injected hydrogen were redistributed into the grain boundaries causing grain boundary decohesion (photo 4a). Prolonging the pre-exposure resulted in more hydrogen diffusing into the samples; also ageing produced a brittle network of  $\eta$  precipitates along grain boundaries. The samples became intrinsically more brittle and therefore the test time was short (approximately 1½ hours) and less hydrogen was injected and redistributed. The samples failed with the 3 regions of fracture, i.e. intergranular rim, cleavage and transgranular core. Dry samples aged up to 6 hours were intrinsically ductile. During the 18 hours of slow straining, a large quantity of hydrogen was injected into the grain boundaries and the grain matrix and thus failed with the three regions of fracture. Age hardening reduced the test time to approximately 6 hours. There was less time to inject hydrogen into the grain boundaries and eventually the samples failed by very ductile grain boundary decohesion (photo 4b). Prolonged ageing caused softening in the grain matrix but formed a brittle network of  $\eta$  precipitates along the grain boundaries. The test time was reduced to about 4 hours. There was less hydrogen injected but it still resulted in ductile grain boundary decohesion. Beyond 120 hours of ageing, the brittle network of precipitates was more pronounced as suggested by thin foil observation. The samples were intrinsically more brittle. There was even less hydrogen injected within the three hours of testing and therefore the samples failed by transgranular fracture. In dry samples, hydrogen injection during testing was the only embrittlement and it was a slow process. These samples survived above the fracture stress level of embrittled samples without failure; thus despite the more intergranular appearance of the dry samples, their fracture stresses and elongations were higher than the corresponding wet samples.

The improvement of hydrogen embrittlement resistance in Al-Zn-Mg alloys by copper or chromium addition is evident, but the embrittlement and the improvement mechanism still require study.

#### 5. CONCLUSIONS AND PROPOSALS FOR FURTHER WORK

The elongation and fractographic studies of the alloys tested at slow strain rates can be explained in terms of hydrogen transport via mobile dislocations ahead of crack tip. Hydrogen lowers grain boundary and lattice energies, causing a decrease in ductility and fracture stress. The addition of copper assists hydrogen recombination and therefore raises total hydrogen intake before failure. The mechanism by which chromium inhibits embrittlement is still not clear and may be related both to hydrogen recombination and to inhibition of hydrogen entry.

Although the slow strain rate technique provides much greater sensitivity to the presence of hydrogen, it does suffer from disadvantages. The problem of uncontrollable local strain rate and crack growth rate, once local plasticity or crack propagation has started, makes detailed interpretation of fractography difficult and it is therefore proposed to carry out true stress corrosion tests on compact tension fracture toughness samples to study crack propagation properties of the alloys, especially the copper-bearing alloy. An autoclave (Fig. 10) has been constructed to permit the use of a flexible range of test piece geometries to be employed both with and without applied load. Also selected slow strain rate tests and dead load tests will be carried out using the existing sheet tensile pieces in order to compare information from these two techniques.

## REFERENCES.

1. L. Christodoulou, PhD thesis, London University, 1980.
2. J.K. Tien, Proc. of the A.I.M.E. Conference on Effect of Hydrogen in Metals, Wyoming, 26-31 August 1982 (edited by I.M. Bernstein and A.W. Thompson), 437, August 1981.
3. J.A. Donovan, Met. Trans. 7A, 1677, Nov. 1976.
4. J.A. Donovan, Met. Trans. 7A, 145, Nov. 1976.
5. J. Albrecht, I.M. Bernstein and A.W. Thompson, Met. Trans. 13A, 811, May 1982.
6. R.N. Parkins, A.S.T.M. Symposium on Stress Corrosion Cracking - The Slow Strain Rate Technique, Toronto 2-4 May, 1977, (edited by G.M. Ugiansky and J.H. Payer), 5, Jan. 1979.
7. G.M. Ugiansky, C.E. Johnson, D.S. Thompson and E.H. Gillespie, (see (6)) 333.
8. H. Buhl (see (6)) 333.
9. J.K. Tien, Proc. of the A.I.M.E. Conference on Effect of Hydrogen on behaviour of Materials, Wyoming, 7-11 September 1975 (edited by A.W. Thompson and I.M. Bernstein), 309.
10. N. Holroyd and D. Hardie, Corrosion Science 21, 129, 1981.

ELONGATION

%

14

12

10

8

6

4

2

0

Al-Zn-Mg

Tensile test result symbols :

■, + wet elongation

⋮, | dry elongation

▲ wet 0.2% proof stress

• wet fracture stress

△ dry 0.2% proof stress

○ dry fracture stress

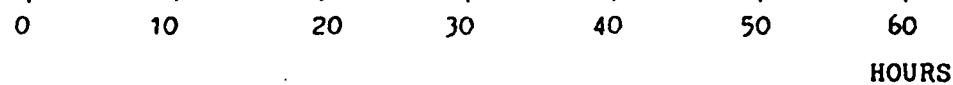


Fig. 1a. Variation of elongation %

STRESS

MNm<sup>-2</sup>

500

400

300

200

100

0

10

20

30

40

50

60

HOURS

Fig. 2a. Variation of 0.2% proof stress and fracture stress.

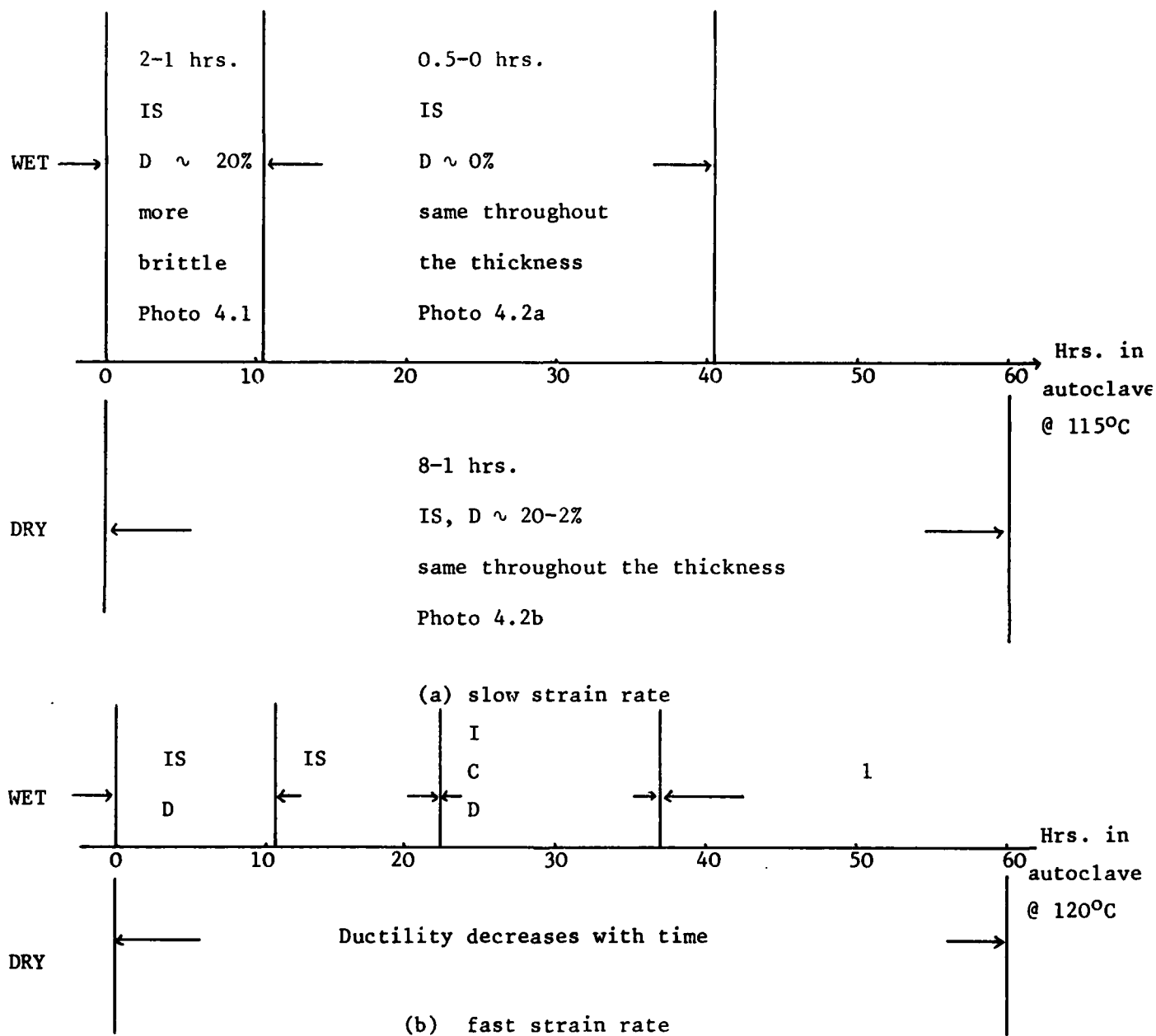


Fig. 3 Variation of fractography with hours in autoclave.

Ternary alloy Al-Zn-Mg

Symbols: I = intergranular                      IS = intergranular with slip marks  
 ID = intergranular ductile                    C = transgranular cleavage  
 D = transgranular ductile

Time shown in each region is the time from yield to fracture

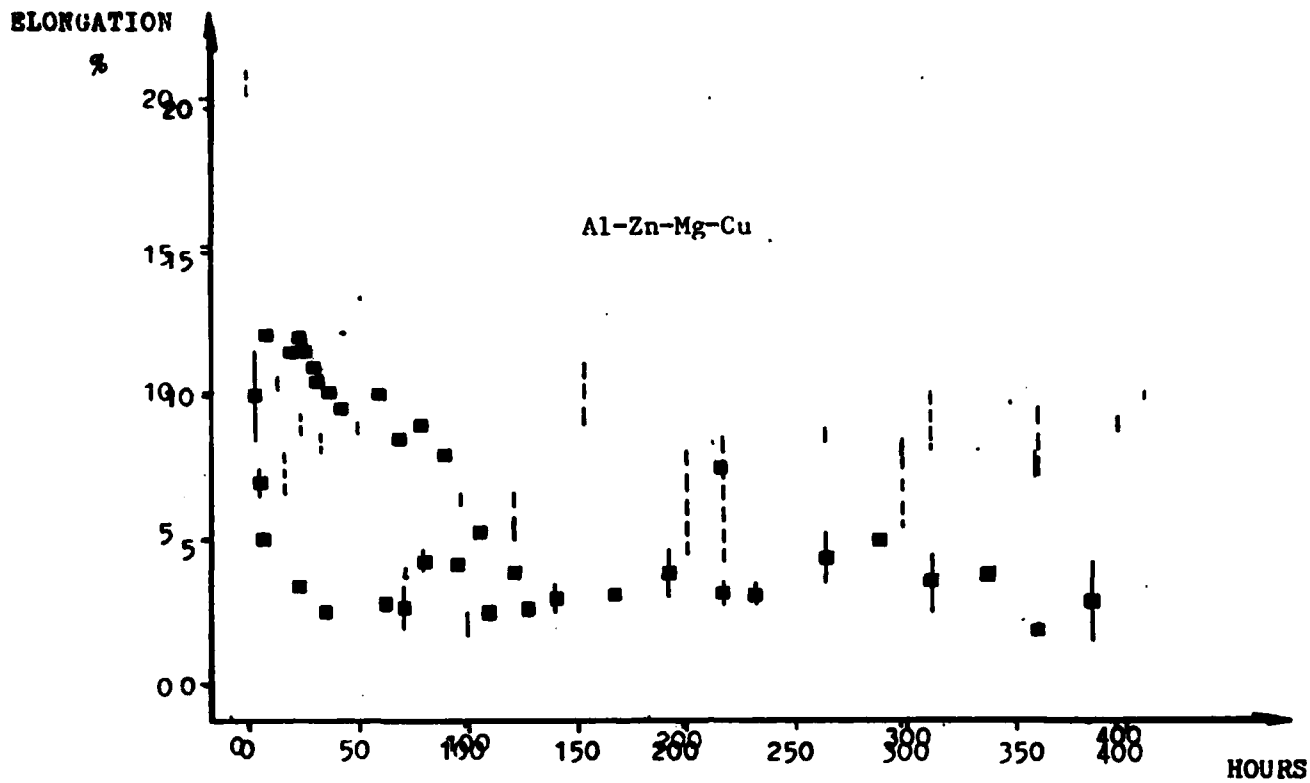


Fig. 4a Variation of elongation %

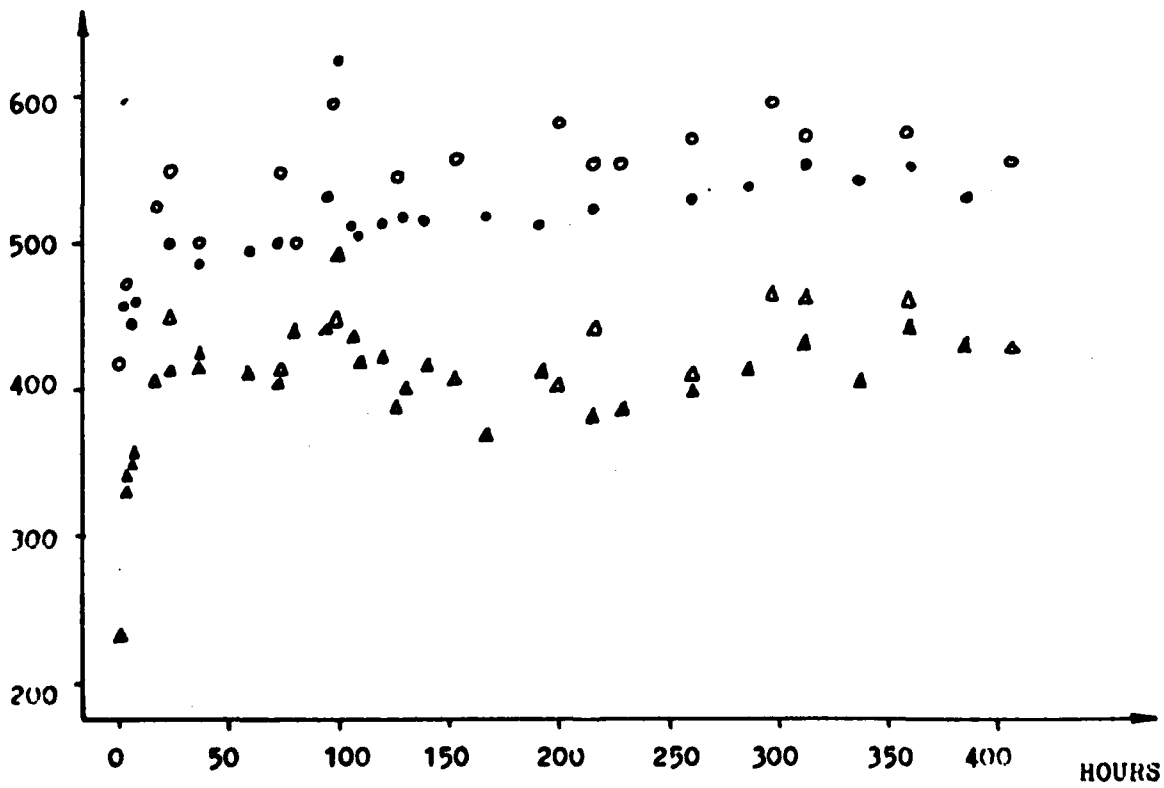
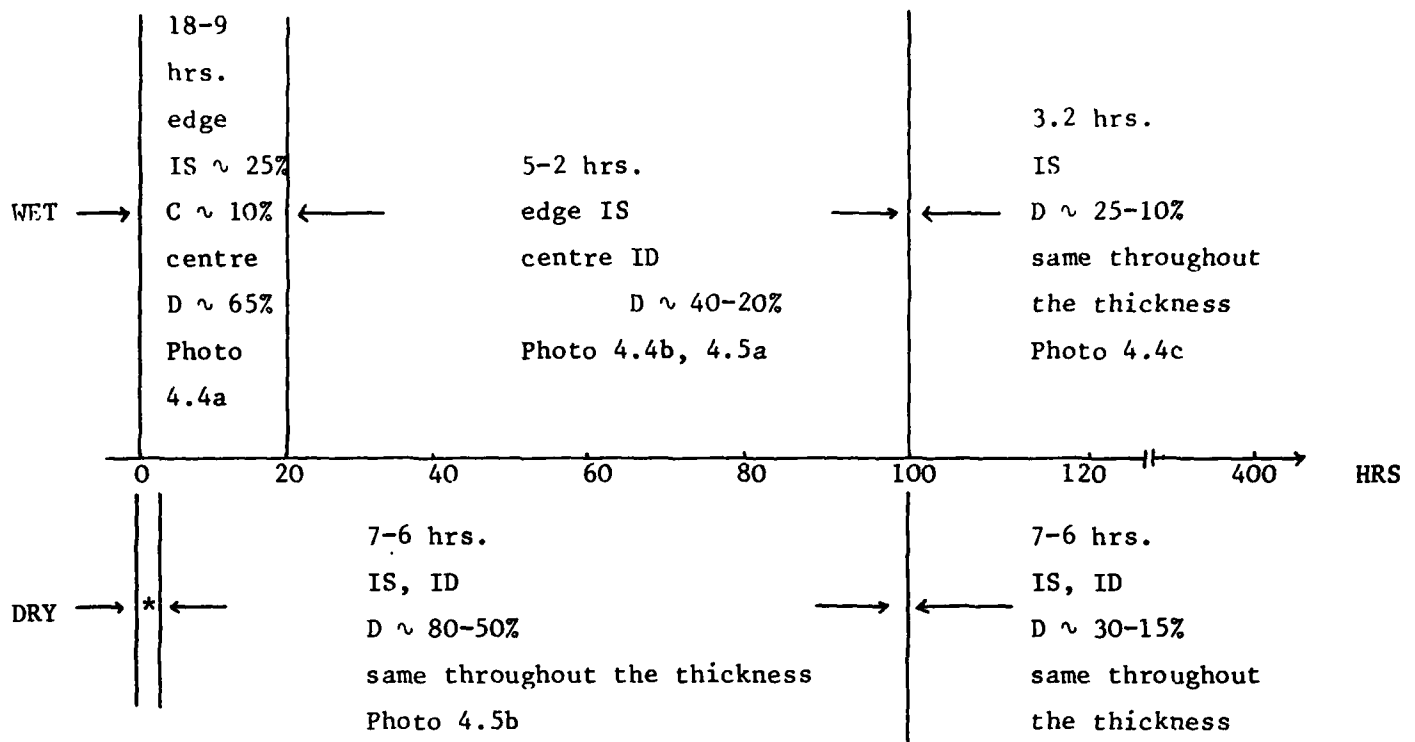


Fig. 5. Variation of 0.2% proof stress and fracture stress



\* 18-9 hrs.  
IS, ID  
D ~ 100-80%

(a) slow strain rate

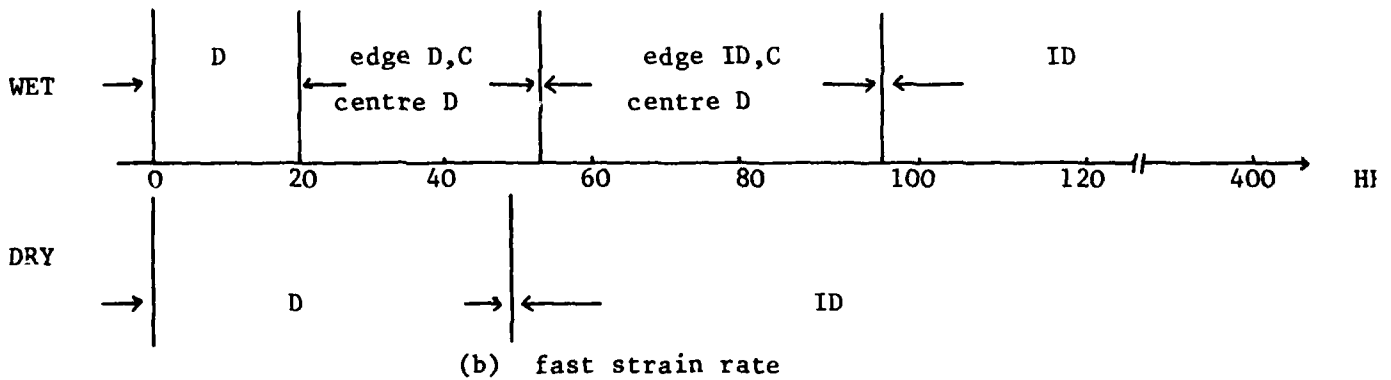
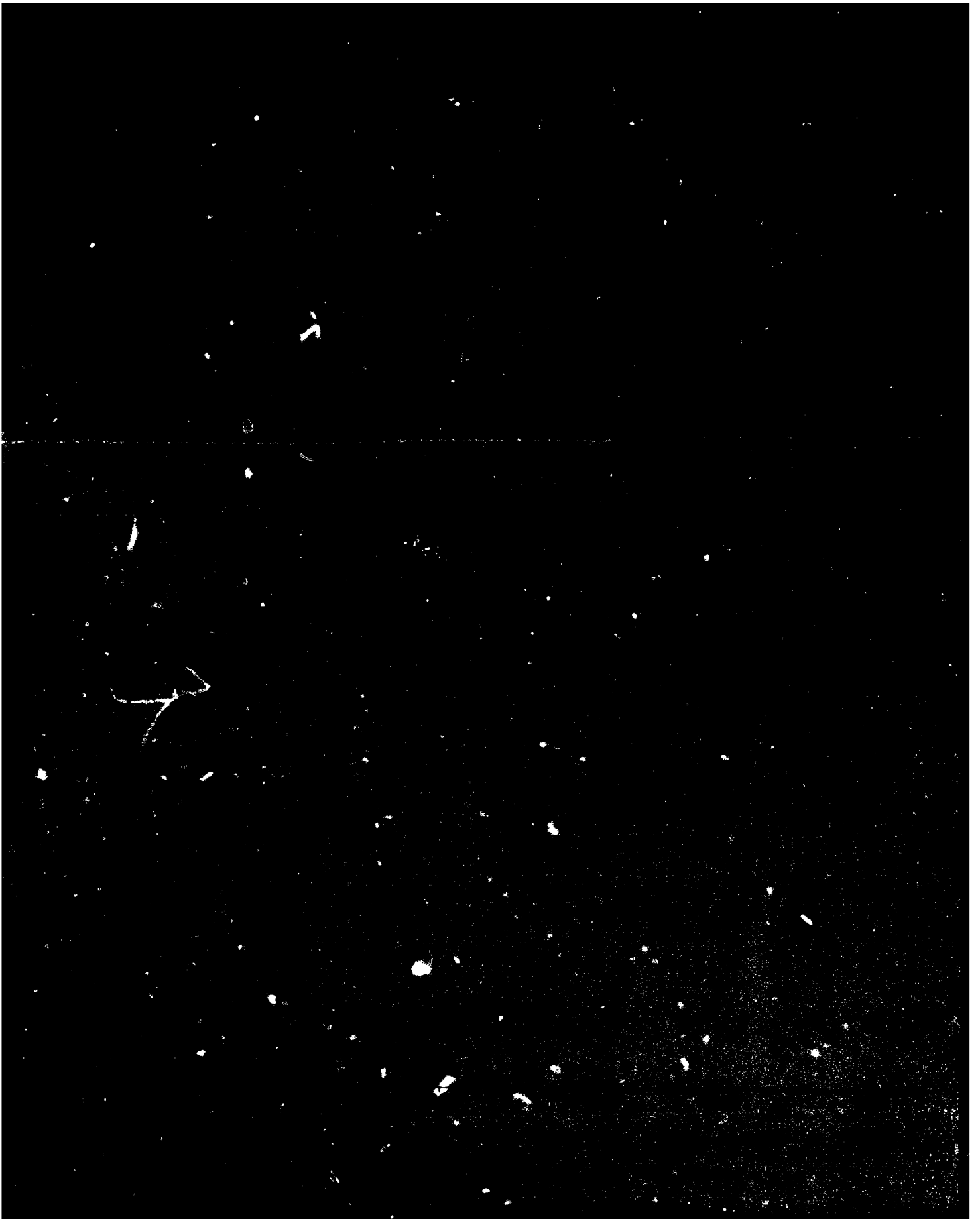
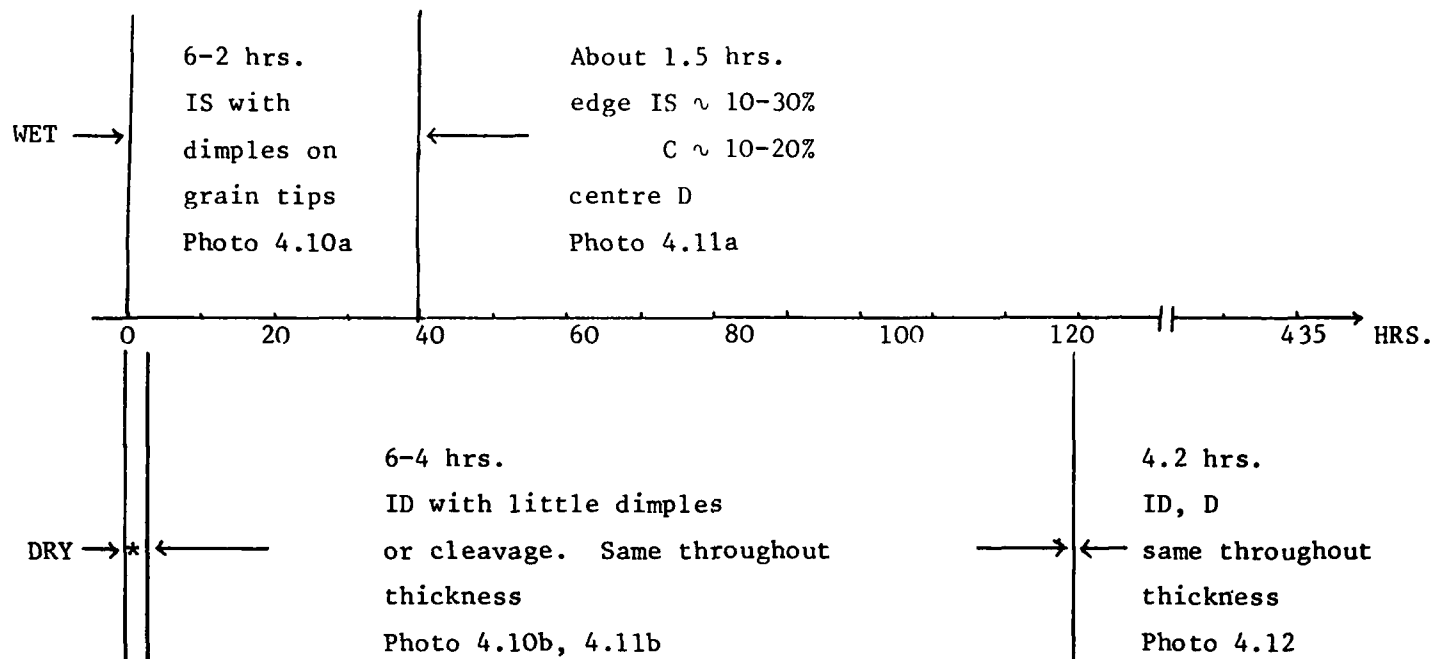


Fig. 6 Variation of fractography with hours in autoclave

Al-Zn-Mg-Cu







\* 20-12 hrs.  
edge ID ~ 10%  
C ~ 30%  
centre D ~ 60%  
Photo 4.9a, b.

(a) slow strain rate

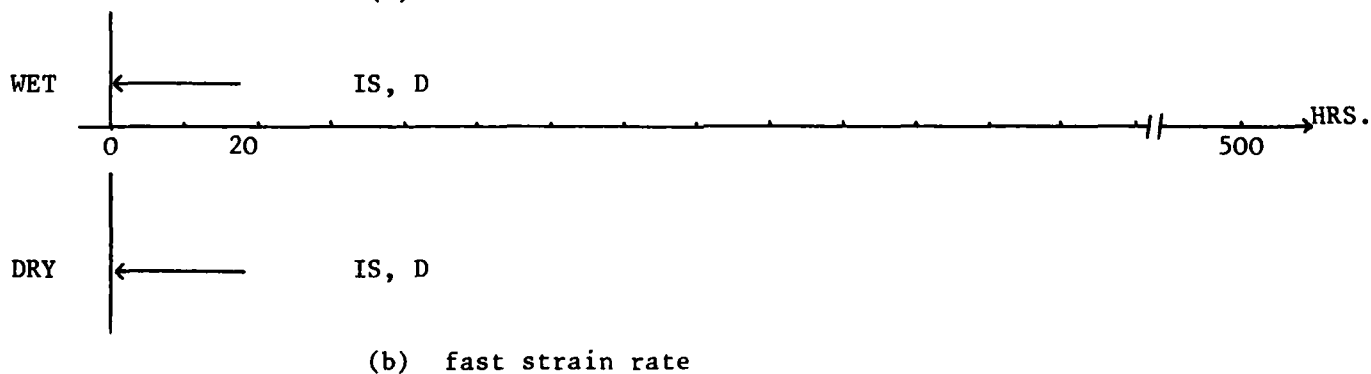
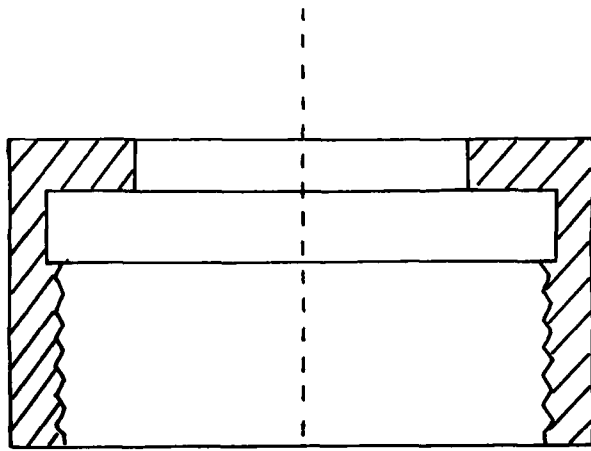


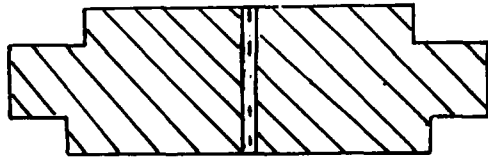
Fig. 9 Variation of fractography with hours in autoclave

Al-Zn-Mg-Cr



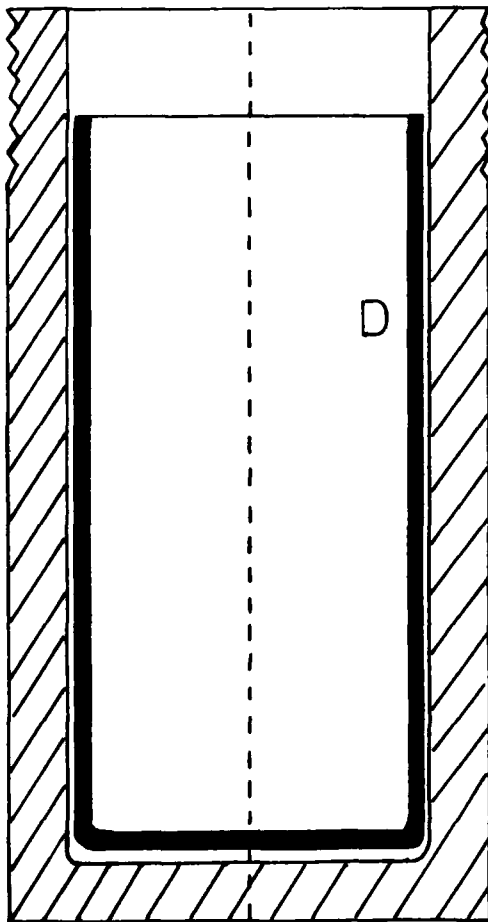
A

A Stainless steel screw cap with tomy base (not shown here)



B

B Aluminium lid (can be adapted to fit thermocouple, pressure valve and test rig, etc.)



C

C Stainless steel container with a heating jacket (not shown here). The temperature is regulated by a Eurotherm control.

D Duran glass beaker to hold water or other corrosive liquid

Fig. 10. Schematic diagram of the autoclave.

Scale: 1cm = 1 inch



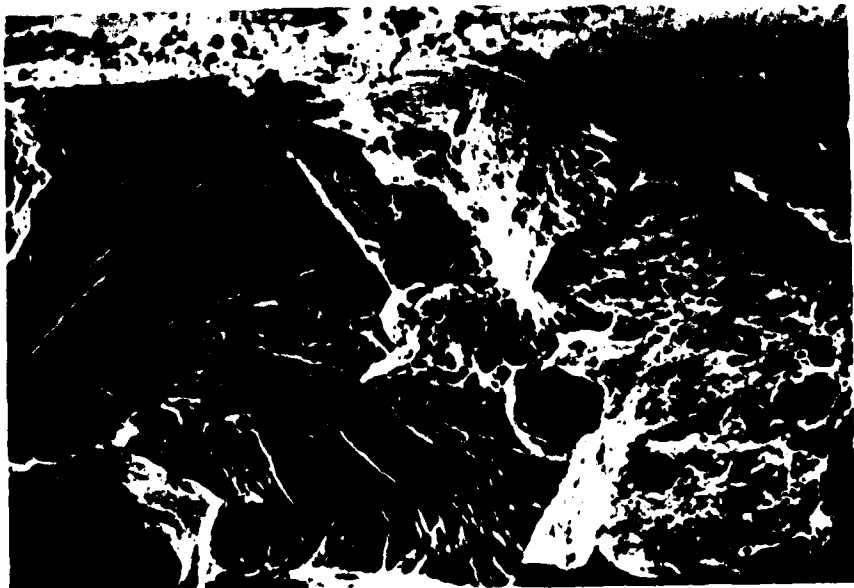


Photo 2, x 820.

Fractograph of a ternary sample pre-exposed for 28 hours. The blisters on the grain boundary surface were caused by exposing the fracture sample to laboratory air for one month.

Photo 3.

Al-Zn-Mg-Cu pre-exposed for 110 hours, shows H<sub>2</sub> bubbles on grain boundaries and in the grain matrix.

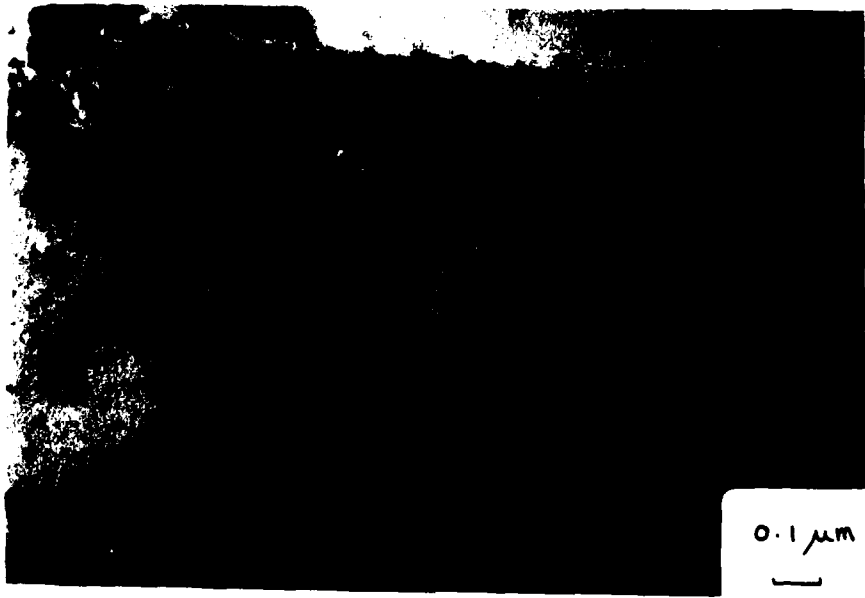
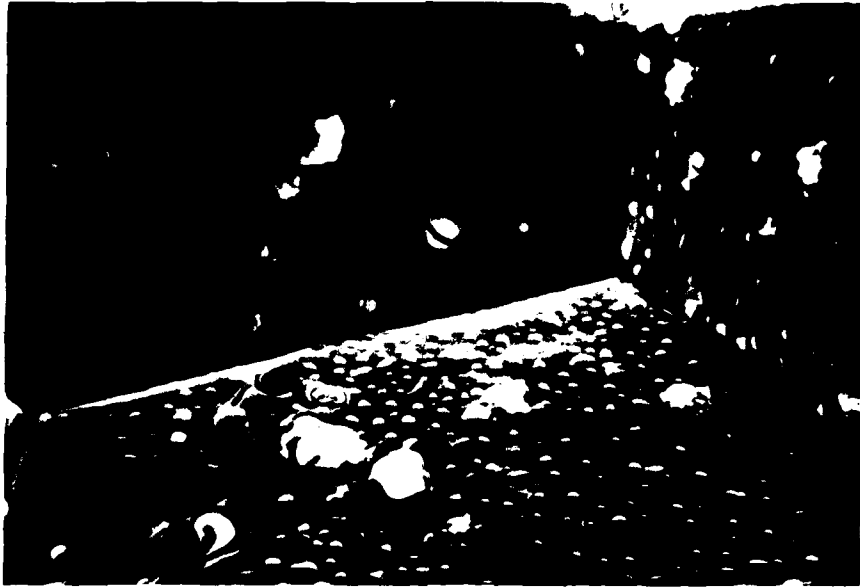


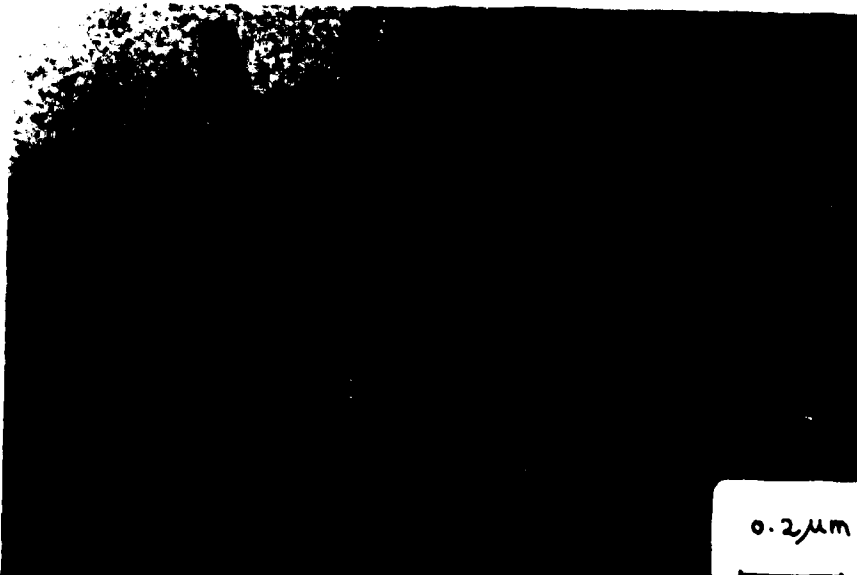
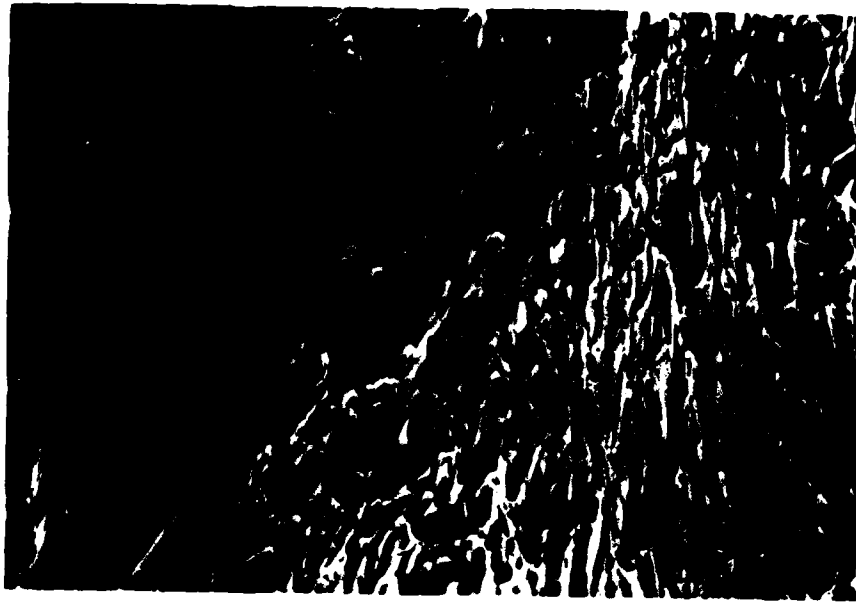
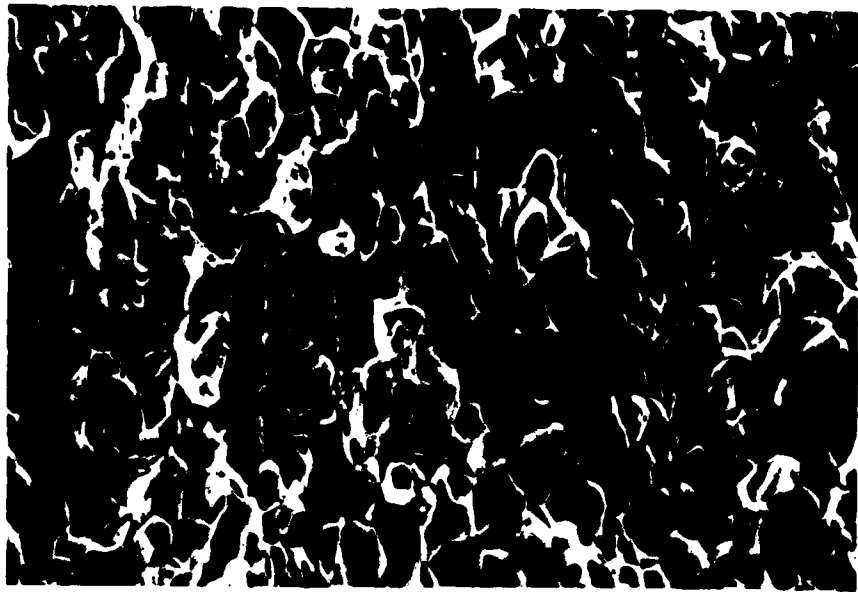
Photo 4 a,b, x 420.  
Al-Zn-Mg-Cr.

(a) Fractograph of a sample pre-exposed for 22 hours; brittle grain boundary decohesion.

(b) Fractograph of a sample dry-aged for 26 hours; very ductile grain boundary decohesion.

Photo 5.

Al-Zn-Mg-Cr pre-exposed for 192 hours; shows H<sub>2</sub> bubbles on the precipitates along a grain boundary.



0.2  $\mu$ m



**END**

**FILMED**

**2-83**

**DTIC**